

Article

Effect of Local Recrystallized Grains on the Low Cycle Fatigue Behavior of a Nickel-Based Single Crystal Superalloy

Xianfeng Ma ^{1,2,*}, Jishen Jiang ¹, Wenjie Zhang ¹, Hui-ji Shi ^{2,*}  and Jialin Gu ³

¹ Sino-French Institute of Nuclear Engineering and Technology, Sun Yat-Sen University, Zhuhai 519082, Guangdong, China; jiangjsh3@mail.sysu.edu.cn (J.J.); zhangwj25@mail2.sysu.edu.cn (W.Z.)

² AML, School of Aerospace, Tsinghua University, Beijing 100084, China

³ Department of Materials Science and Engineering, Tsinghua University, Beijing 100084, China; gujl@mail.tsinghua.edu.cn

* Correspondence: shihj@mail.tsinghua.edu.cn (H.S.); maxf6@mail.sysu.edu.cn (X.M.)

Received: 29 April 2019; Accepted: 11 June 2019; Published: 18 June 2019



Abstract: This paper aims to understand the effect of local recrystallization (RX) on the low cycle fatigue fracture of a turbine-blade single crystal nickel-based superalloy. The fatigue life of the single crystal superalloy was evidently decreased by local recrystallization. In single crystal specimens, casting porosity is the preferential fatigue crack initiation site, which is followed by crystallographic crack propagation along one or several octahedral slip planes. For all RX specimens, fatigue cracks preferred to initiate from local recrystallized grains and propagated through the recrystallized grains in a transgranular manner, followed by crystallographic crack propagation in the substrate single crystal superalloy. Moreover, fatigue tests indicated that locally recrystallized specimens exhibited temperature dependent fracture modes, i.e., transgranular cracking dominated at 550 °C, whereas intergranular cracking was preferred at 850 °C. Evident oxidation of fracture surfaces and strength degradation of grain boundaries at 850 °C was evidenced by scanning electronic microscopic observations. The present study emphasized the need to evaluate the effect of recrystallization according to the working conditions of turbine components, i.e., the local temperature.

Keywords: nickel-based superalloy; fatigue; recrystallization; microstructure; temperature

1. Introduction

Due to its excellent mechanical properties under elevated temperatures, single crystal (SX) and directionally solidified (DS) superalloys, with the elimination of transverse grain boundaries, have been widely used as the primary materials for turbine blades [1]. However, single crystal superalloys usually have removed grain boundary (GB) strengthening elements, making them sensitive to any transverse boundaries or defects, e.g., recrystallization [1,2]. With increasing attention on the safety of turbine engines in recent decades, there have been more and more studies on the recrystallization issue of turbine alloys, i.e., SX and DS superalloys [3–6]. It has been reported that recrystallization (RX) grains can act as the preferred fatigue crack initiation sites of turbine blades [1,7]. So far, little research has been done regarding the effect of RX on the fatigue behavior of SX superalloys [8], aside from the limited studies on directionally solidified (DS) alloys [9–11]. There are still some basic questions to be answered; for instance, the effect of temperature on the fracture mode of recrystallization region has been rarely discussed [9]. To the author's knowledge, the conditions that control if the partial recrystallization is fatal or insignificant remain unclear. Bürgel's [8] early work on a recrystallized single crystal superalloy at 950 °C showed no evident influence of recrystallization on the fatigue crack initiation life, except for a higher crack density. In previous studies, the present authors found

that the low cycle fatigue life of a single crystal superalloy was remarkably reduced at 550 °C by a 150 µm recrystallized layer, up to an order of magnitude [2]. The studies on directionally solidified DZ4 superalloy [10,12] also indicated a significant decrease in fatigue life by recrystallized grains. In contrast, a recent study [13] reported an abnormal increase of fatigue life for DZ4 alloy with recrystallized layer generated by high pressure shot peening and annealing, in which the compact recrystallized layer with refined grains, and annealing twins are perceived to benefit fatigue performance of the superalloy. It is likely that the recrystallization effect is dependent on recrystallization grain microstructures and testing conditions. A study on the Al-Cu-Mg alloy showed that dynamic recrystallization can increase fatigue life in the plastic region and decrease it in elastic region, with recrystallization occurring in the entire sample [14]. To simulate the actual recrystallization microstructure in turbine blades, i.e., discrete recrystallized grains, local recrystallization was specially prepared in this work, using indentation and annealing instead of continuous recrystallized grains/layer as used in most studies [9–11].

In this study, the effects of local recrystallization on the low cycle fatigue behavior of a gas turbine single crystal superalloy were studied. Strain-controlled fatigue tests were performed on both the original SX and locally recrystallized SX samples to reveal the effects of recrystallization. Special attention is placed on examining the fatigue failure mechanism of the recrystallized specimen and the effect of temperature on the fatigue fracture mode.

2. Materials and Experimental

The material used is a single crystal nickel-based superalloy with a nominal composition (in wt.%) of 0.067 C, 3.9 W, 12.0 Cr, 9.0 Co, 1.9 Mo, 4.0 Ti, 3.6 Al, 5.0 Ta, and balanced Ni. Single crystal rods were directionally solidified to produce a [001] crystal orientation. The as-received superalloy has a two-phase microstructure, consisting of a face centered cubic (FCC) γ phase and a precipitated γ' phase (Figure 1). The γ' precipitates have a volume fraction of about 80%. Some Ta-rich carbides are widely distributed [15] and eutectic is noticed occasionally in the alloy (Figure 1). The fatigue sample has a total length of 85 mm and a gage length of 15 mm, as shown in Figure 2a,b. A special procedure was adopted to prepare fatigue samples with local recrystallized grains. The fatigue specimen gage section has an initial diameter of 7 mm. A brinell indentation of 500 kgf was used to introduce local plastic deformation on a pre-machined platform within the gage length, and local recrystallization was formed in the subsequent solution heat treatment. Then, the pre-machined platform was removed, and the specimen was gradually machined to the final cylindrical diameter of 6 mm. The local recrystallized region has a depth of 1.8 mm and a length of 3 mm, which will remain after machining. The detailed microstructure of the local recrystallization region was examined under optical microscope, as shown in Figure 2c. It was composed of multiple small grains, and twins were evidently observed.

The fatigue tests were performed under a SHIMAZU EHF-EA10 (Kyoto, Japan) servo-hydraulic fatigue testing machine. A furnace with resistance coils was used to heat the specimen up to 550 °C, and three adjustable thermocouples were employed to monitor and control the temperature within about ± 1 °C. Fully reversed fatigue tests were controlled by the strain with a triangle waveform, following the ASTM standard for a strain-controlled fatigue test [16]. An extensometer with a 12.5 mm gauge length was used for fatigue tests. A strain rate of 10^{-3} /s was used for all fatigue tests. A Quanta 200F (Hillsboro, United States) scanning electronic microscope (SEM) was used for the fractography and microstructure analysis of all samples.

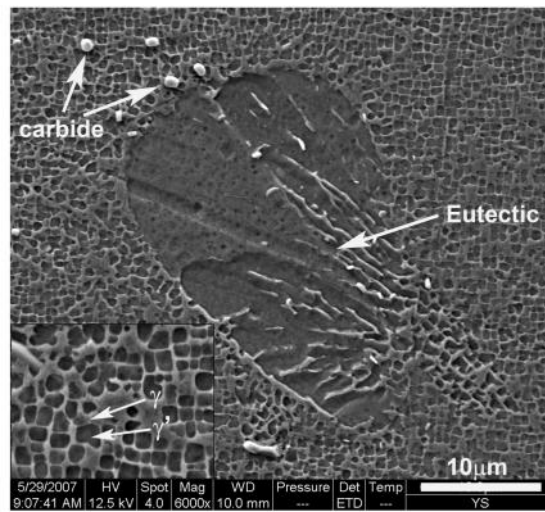
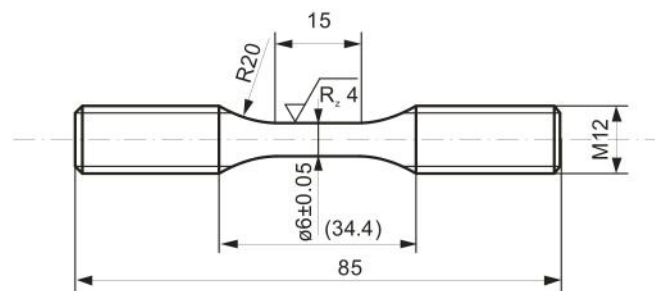


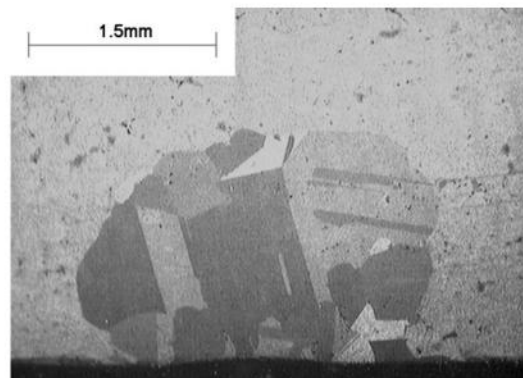
Figure 1. Typical microstructure of a single crystal superalloy under scanning electronic microscope, consisting of γ and γ' phases, carbides, and eutectic.



(a)



(b)



(c)

Figure 2. Single crystal fatigue test samples: (a) specimen dimensions; (b) specimens appearance; (c) optical microstructure of the local recrystallized grains generated by indentation and annealing.

3. Results and Discussion

3.1. Fatigue Fracture Life

Figure 3 shows the fatigue life results of the original single crystal samples and those with local recrystallized grains at two typical strain amplitudes. Normalized strain amplitude (ε_n) was defined as the experimental strain amplitude (ε) divided by a reference strain, i.e., $\varepsilon_n = \varepsilon/100\varepsilon_u$, where the strain (ε_u) corresponds to the ultimate tensile strength of this SX superalloy. It is seen that fatigue life decreases with increasing strain amplitude for both types of samples. Moreover, local recrystallization evidently decreased the fatigue life of the single crystal superalloy. Taking the samples at a high strain amplitude of 0.7%, in Figure 3 for instance, fatigue life of the RX sample was reduced to about 1/3 of that of the original SX alloy. At a lower strain amplitude (0.6% in Figure 3), the degradation of fatigue life by local RX becomes even more evident, being about an order of magnitude lower. The present study is consistent with those reporting on a single crystal superalloy with a 150 mm recrystallized layer [2]. Previous studies on directionally solidified superalloys, e.g., DZ4 and DZ40M, with uniform recrystallized layers exhibited a similar drop in fatigue life [10,11].

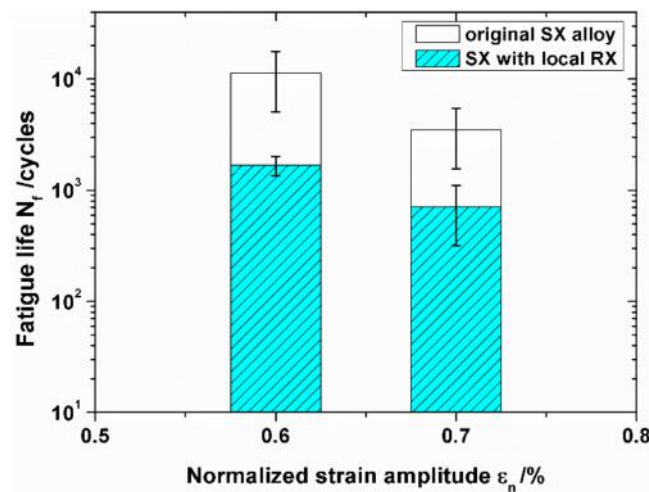


Figure 3. The effect of local recrystallization on the low cycle fatigue life of a single crystal superalloy.

3.2. Fatigue Fractography and Fracture Mechanism

All the fatigue fractured samples were subjected to fractographic analysis under a scanning electronic microscope. Figures 4 and 5 show the fracture surfaces of original single crystal samples. Figure 4a shows the typical fracture surface of a single crystal superalloy fractured after 4889 cycles. It is seen that the specimen showed evident crystallographic fracture, with ridges formed by several {111} slip planes. An examination at higher magnification showed that fatigue crack initiation occurred at a cluster of casting pores, as in Figure 4b. This fatigue failure mode was also commonly observed in the low-cycle fatigue study of the same single crystal alloy at 600 °C [15], indicating that it is the dominant fracture mechanism at lower temperatures. Figure 5a shows the fracture surface of the single crystal sample under a lower strain amplitude ($\varepsilon_n = 0.6\%$), fractured at 15855 cycles. Multiple {111} slip planes were evidently observed and river patterns, associated with crystallographic crack propagation, were noticed. A careful examination under high magnification indicated that multiple crack initiation sites were all associated with cluster of porosity (Figure 5a,b), which is consistent with the result in Figure 4.

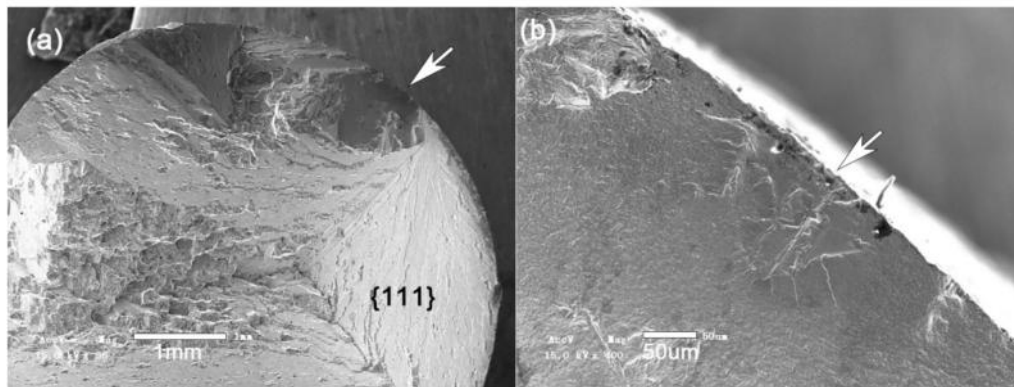


Figure 4. The original single crystal superalloy exhibited a crystallographic fracture mode at 550 °C ($\epsilon_n = 0.7\%$, $N_f = 4889$ cycles): (a) overall fracture surface; (b) crack initiation at casting porosity.

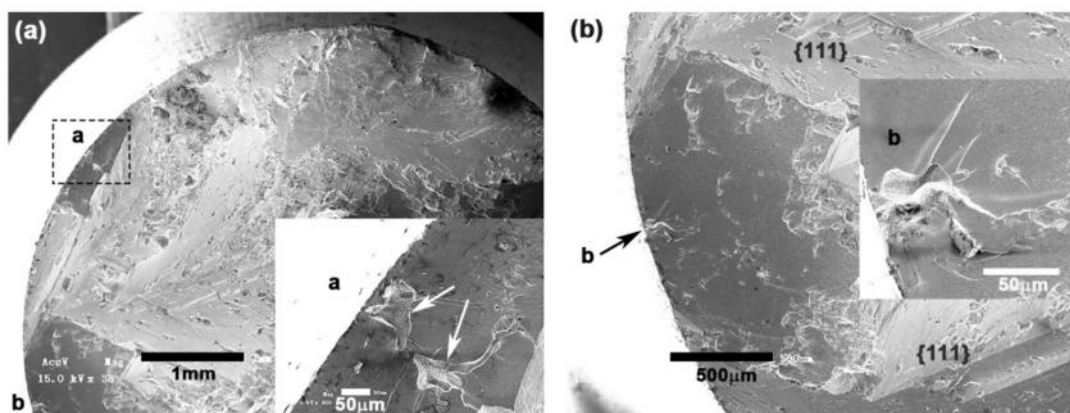


Figure 5. Original single crystal superalloy exhibited crystallographic fracture mode at 550 °C ($\epsilon_n = 0.6\%$, $N_f = 15855$ cycles): (a) overall fracture surface; (b) crack initiation at casting porosity.

For specimens with local recrystallization, Figure 6a shows that the primary fatigue crack initiation site was at the recrystallized region (marked by an ellipse). The higher magnification observation in Figure 6b reveals that the crack initiation was caused by recrystallized grains, which appeared different from those in Figures 4 and 5. Moreover, it should be noted that recrystallized grains show a transgranular fracture mode, which is distinct from the intergranular fractures widely reported in the literature [10,11]. Examination of other secondary initiation sites (marked by arrows in Figure 6a) is shown in Figure 6c, indicating the casting pores caused microcracks [15]. The crack propagation plane in Figure 6a is about 50° inclined to the loading axis, which is identified to be a {111} slip plane [15]. Details of the crystallographic fracture along the {111} planes can be seen clearly in Figure 6d.

Figure 7a is another example of locally recrystallized single crystal sample after fatigue fracture. The crack initiation region is related to the recrystallized grains, as shown in Figure 7b. Nonuniform fracture features (Figure 7b) were unlike those observed in the single crystal superalloys in Figures 4 and 5. A higher magnification examination of the crack initiation site revealed a surface defect or dent (marked by '1') in Figure 7c. The one marked by '2', showing casting pores, was revealed on the {111} slip plane. Figure 7d ('d' in Figure 7b) and Figure 7e ('e' in Figure 7b) show the crack propagation behavior adjacent to the crack initiation site before proceeding along the {111} plane. Striations can be identified in Figure 7d,e, in which the striations are perpendicular to the crack propagation direction (denoted by 'c.p.d.'). This striation feature was commonly observed in polycrystalline alloys and rare in single crystal superalloys.

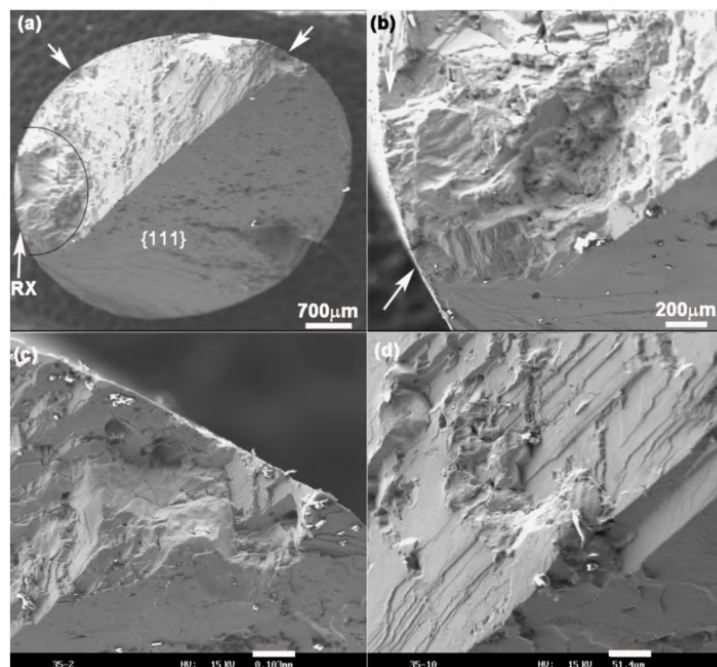


Figure 6. Fracture surface of SX alloy with local recrystallization at 550 °C ($\epsilon_n = 0.7\%$, $N_f = 988$ cycles); (a) fracture surface; (b) crack initiation site; (c) secondary fatigue crack initiation site; (d) slip deformation and river patterns on {111} slip planes.

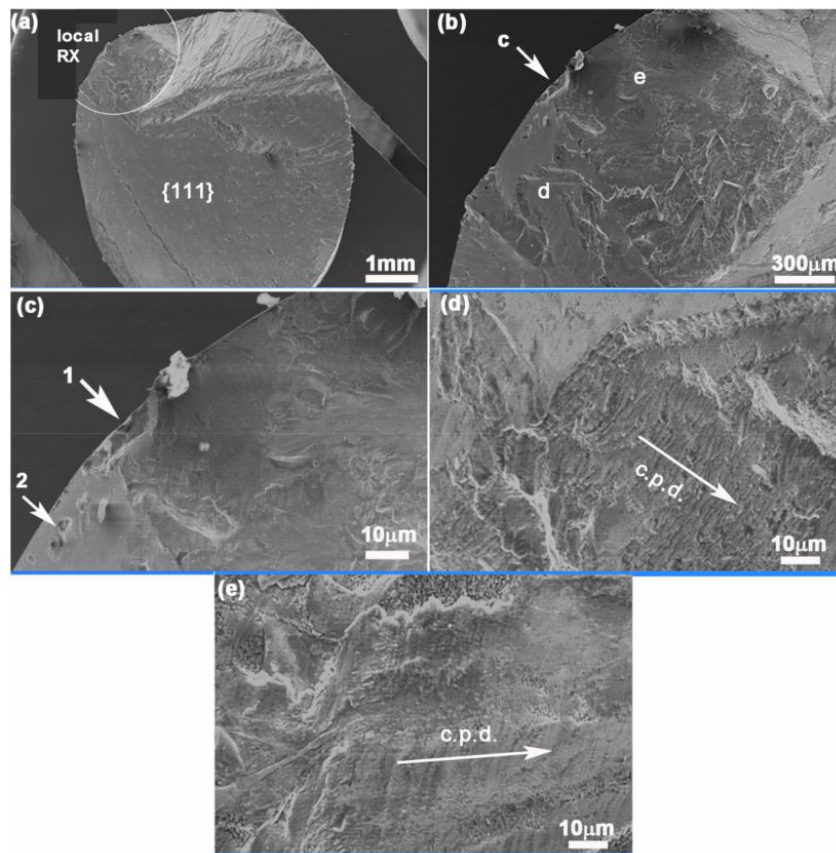


Figure 7. Fracture surface of a single crystal alloy with local recrystallization at 550 °C ($N_f = 2757$ cycles); (a) overall fracture surface; (b) crack initiation and propagation region; (c) crack initiation site; (d) crack propagation behavior at site 'd'; (e) crack propagation behavior at site 'e'.

Figure 8a shows the microstructure of the longitudinal section of the specimen in Figure 6, where annealing twins were observed, and the local recrystallized region was measured to be about 1.1 mm deep. In Figure 8b, transgranular cracking of recrystallization grains was evident, and no fracture of RX grain boundaries was noticed. Figure 8c shows a higher magnification of annealing twins in the local recrystallization region, which is similar to that observed in Figure 2c. Figure 8d is a high magnification of the $\gamma + \gamma'$ phase in the recrystallized grain, showing morphological changes due to microstructural deformation. Regarding the effect of recrystallization on fatigue life, the primary difference comes from the crystal orientations of the alien RX grains compared to the $\langle 001 \rangle$ orientation of the original SX superalloy, which will lead to higher localized stress and, hence, a larger cyclic plastic strain in the RX region. This is also confirmed by a recent crystal plasticity simulation study on the influence of local RX grains on the fatigue life of a directionally solidified superalloy [17].

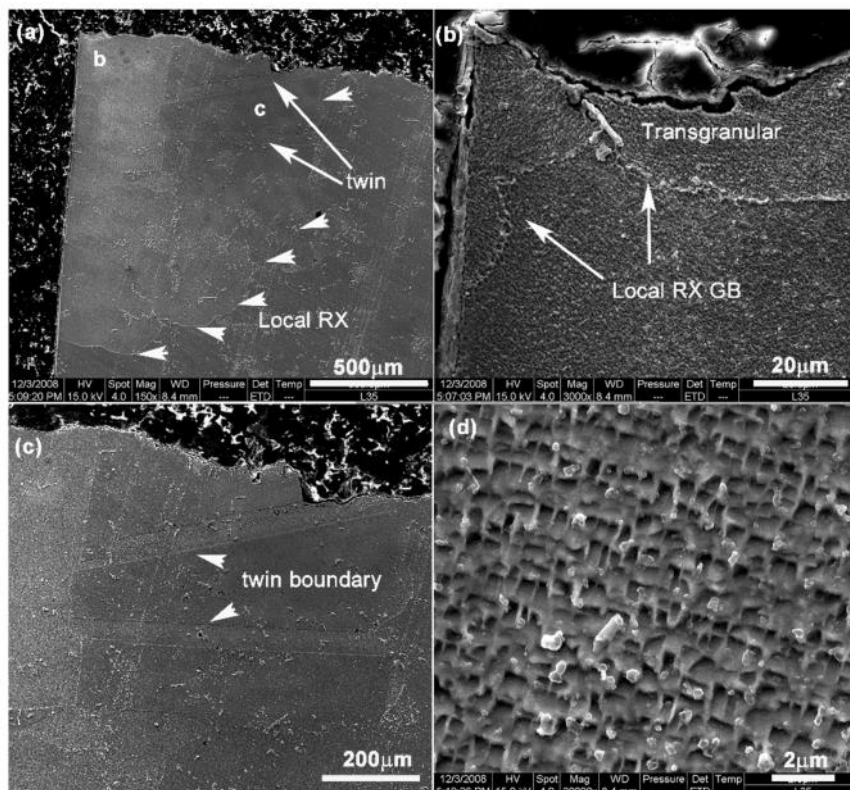


Figure 8. Longitudinal section microstructure of the SX alloy with local recrystallization at 550 °C ($\epsilon_n = 0.7\%$, $N_f = 988$ cycles); (a) overview; (b) transgranular fracture of recrystallized grains; (c) annealing twins in local recrystallized grains; (d) deformed microstructure in recrystallized grain.

3.3. Temperature Effect on the Fatigue Fracture Mechanism

Previous studies on directionally solidified DZ4 alloys [13] found that transgranular fracture would be prevalent at an intermediate temperature, e.g., 350 °C. It was suggested by the present authors that testing conditions (e.g., temperature) might play an important role in the fracture mode of recrystallized grains. However, to the best of our knowledge, there has been no experimental research on single crystal superalloys to verify it. Hence, a control test was done on a locally recrystallized SX sample at higher temperature, e.g., 850 °C. Figure 9a shows the overall fracture surface after fatigue failure, showing primary crack initiation at the local RX grains. The crack propagation region of the fracture surface appears approximately flat, indicating a non-crystallographic Mode-I fracture, with no $\{111\}$ slip planes observed. By examination under higher magnification in Figure 9b, an oxidized layer was evident on the fracture surface, in contrast to the fracture surfaces in Figures 6 and 7. Figure 9c is a high magnification of Site 'c' in Figure 9a, revealing a secondary cracking manner, which will be

further examined in Figure 10. Figure 9d shows the fracture in the fast rupture region ('d' in Figure 9a), indicating no dimples but small facets, which were also observed in the fracture of the single crystal superalloy at 850 °C [15].

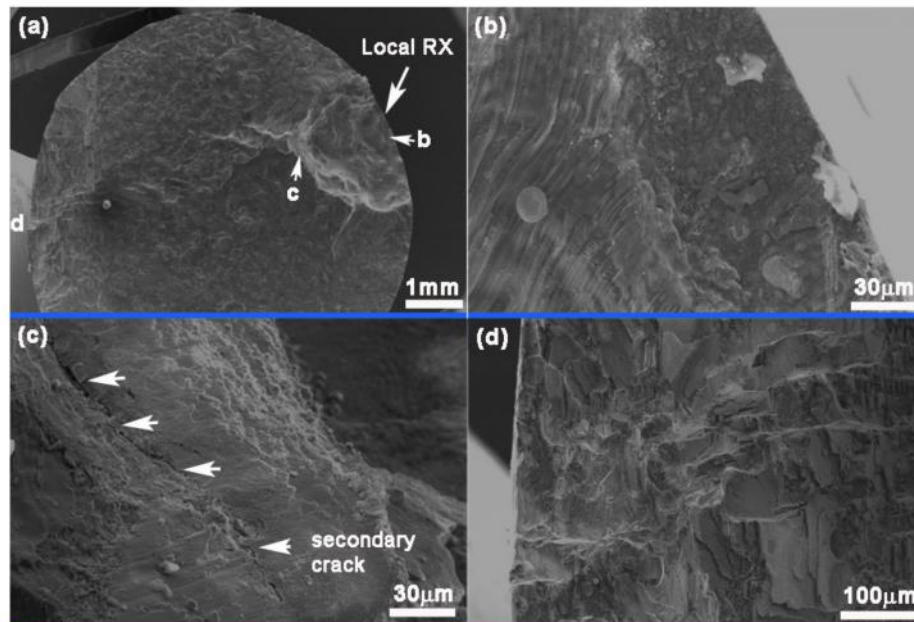


Figure 9. Fatigue fracture of a single crystal alloy with local recrystallization at 850 °C ($N_f = 5235$ cycles) (a) overview of fracture surface; (b) surface oxidation; (c) secondary cracking; (d) fracture at a high ΔK region.

The sample in Figure 9 was sectioned longitudinally to better understand the fracture mechanism at 850 °C. Figure 10a shows, at the recrystallized region, the primary crack and secondary crack, which were identified to be intergranular cracking. In Figure 10b, the oxidized layer is observed on the cracked grain boundary ('GB', arrowed). Figure 10c examines the secondary cracks at a higher magnification, indicating that the fatigue crack preferentially propagated along the grain boundaries (GBs), assisted by oxidation. Figure 10d clearly shows the oxidation of the triple joints of the grain boundaries. For the studied SX superalloy without GB-strengthening elements (e.g., B, Hf, and Zr), oxidation has an evident effect on the cracking of the recrystallized grain boundaries. At 850 °C, transverse recrystallized grain boundaries act as a crack initiation site, due to the local stress raise related to the oxidation and opening of the grain boundary. With cyclic loading, fatigue crack propagation was assisted by the penetration of oxidation along the grain boundary and the alternant cracking of the grain boundary. Previous studies [18] indicated that Ni, Al, and Ti atoms will be consumed by oxygen and transformed into NiO, Al₂O₃, and TiO₂ oxides, leading to a γ' dilution zone due to lack of Al and Ti elements, which can further reduce the local strength of the grain boundary ahead of the crack tip. EDS analysis confirmed the concentration variation of Ni, Cr, Ti, and Al elements near the intergranular crack.

In Figure 10c, a branch of the crack was arrested by a blocky carbide, indicating the impeding effect of carbide on oxidation assisted intergranular cracking (marked by arrow). Another example of carbide interaction with a crack is shown in Figure 10e, indicating the barrier effect of blocky carbide. EDS analysis indicated that the fine carbides were rich in Cr, suggesting M₂₃C₆ type carbides [19], which were commonly found along the recrystallized grain boundaries. Previous studies [20,21] reported the beneficial effect of M₂₃C₆ carbides on fatigue and creep properties, via a GB strengthening effect, the prohibition of GB immigration, and the pinning of dislocation. It is also suggested that Cr and Al elements in carbides consume part of the oxygen at the crack tip to protect the grain boundary and, on the other hand, reduce intergranular crack propagation by a blunt crack mechanism via carbide fracture to reduce the local stress concentration, as shown in Figure 10c,e.

In Figure 10f, intergranular cracks occurred in the interior of sample, with the crack mating surfaces appearing clean, which indicates that intergranular cracks can still occur without the assistance of oxidation. The observations herein suggest that the intergranular fracture mode at 850 °C is attributed to both aspects: (i) the oxidation assisted brittleness and cracking of GB due to lack of GB-strengthening elements; and (ii) the decrease of GB strength at higher temperatures, which is similar to polycrystalline alloys [13]. It is well known that in polycrystalline alloys, there is a so-called iso-strength temperature, T_E , at which the grain and GB have equal strength [13] (see Figure 11). Hence, it is suggested that there is a critical temperature in the fracture of the recrystallized SX superalloy [9], i.e., intergranular cracking dominates above the temperature T_E , whereas transgranular fracture would be expected below T_E ($550\text{ °C} < T_E < 850\text{ °C}$ for this SX superalloy).

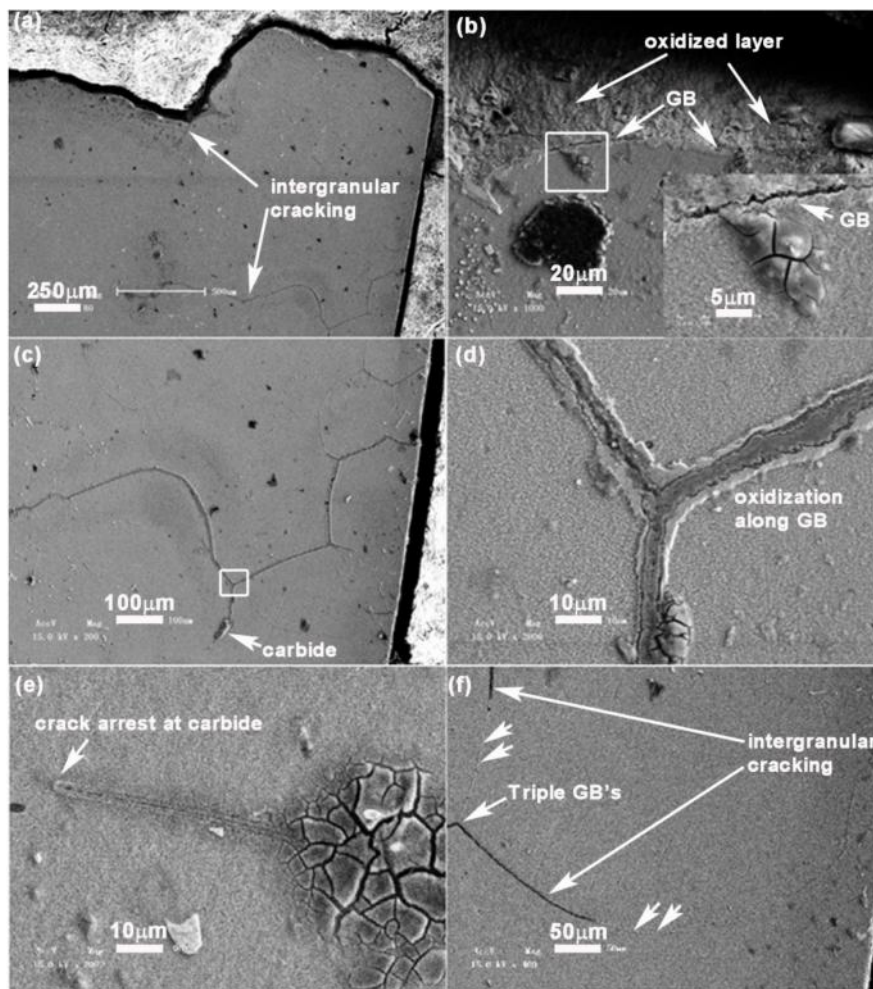


Figure 10. Fracture features on the longitudinal section of the single crystal superalloy with local recrystallization at 850 °C ($N_f = 5235$ cycles): (a) overview; (b) grain boundary ('GB') on the fracture surface; (c) intergranular cracking; (d) oxidation of GB; (e) crack arrested by carbide; (f) cracking of GBs in vacuum.

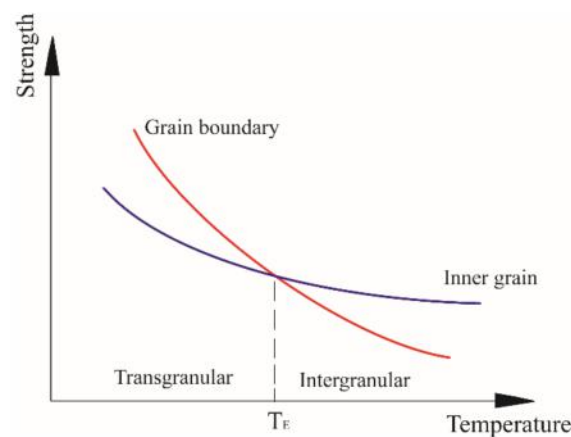


Figure 11. Schematic temperature-dependent fracture: transgranular versus intergranular.

Regarding the fatigue fracture of SX alloy with local RX effect in this study, a schematic graph was provided in Figure 12 to summarize the fatigue fracture behavior in a different temperature regime. Figure 12a shows the prevailing transgranular fracture at lower temperatures, i.e., $T < T_E$, e.g., 550 °C, where fatigue cracks preferentially initiate from casting defects in the local RX region. The crack propagation in the single crystal matrix proceeds along one or several octahedral slip planes [15]. Figure 12b shows the intergranular fracture mode at higher temperatures, i.e., $T > T_E$, e.g., 850 °C. In this case, fatigue crack was assisted by the oxidation and degradation of grain boundary. After penetrating the RX region, a fatigue crack in the single crystal matrix occurred via multiple wavy slips, exhibiting a macroscopic Mode-I fracture [15]. For a turbine blade, it is known that the temperature profile varies from the top to the root [7], hence the present study emphasizes that it is of practical significance to evaluate the influence of recrystallization according to the local temperature of turbine components in the safety evaluation procedure.

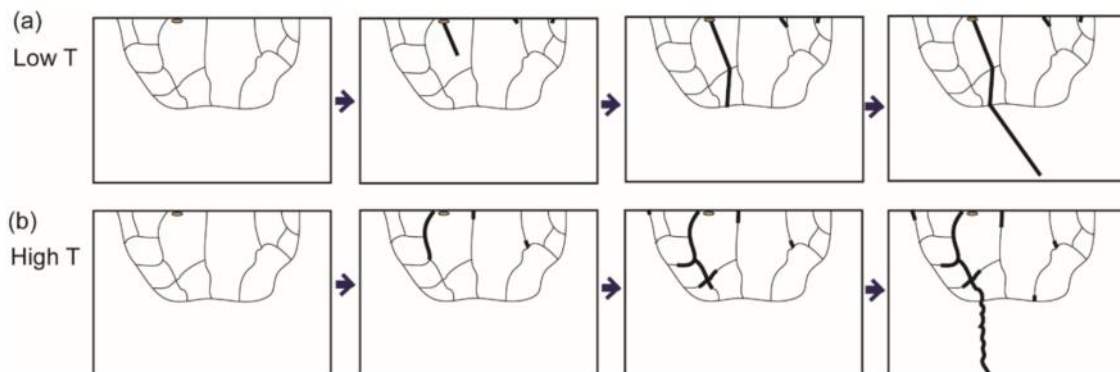


Figure 12. Schematic fatigue fracture modes of the partially recrystallized single crystal superalloy at different temperatures; (a) lower temperature, below T_E , e.g., 550 °C; (b) higher temperature, above T_E , e.g., 850 °C.

4. Conclusions

This study showed that local recrystallized grains evidently decreased the low-cycle fatigue life of a single crystal superalloy at elevated temperatures. For the original single-crystal superalloy samples, fatigue crack initiation at the casting porosity was commonly observed. For all recrystallized samples, fatigue cracks primarily initiated from local recrystallization grains. The recrystallized samples showed a transgranular fracture of recrystallized grains at 550 °C followed by crystallographic cracks along the slip planes in the substrate single-crystal superalloy, instead of intergranular cracking along the recrystallization grain boundaries. The check test at 850 °C showed the widely-reported

intergranular cracking in the local recrystallization region, followed by a Mode-I fracture in the substrate single-crystal superalloy. Hence, this study, for the first time, provides experimental evidence for the temperature-dependent fatigue fracture mode of a single crystal superalloy with partial recrystallization.

Author Contributions: Conceptualization, X.M. and H.S.; methodology, J.J., D.W. and J.G.; investigation, J.J. and D.W.; resources, X.M. and H.S.; data curation, J.J., D.W. and X.M.; writing—original draft preparation, X.M., J.J. and D.W.; writing—review and editing, X.M. and J.J.; supervision, X.M. and H.S.; funding acquisition, X.M. and H.S.

Acknowledgments: The authors acknowledge the support from Guangdong Education Department Fund 2016KQNCX005, 2016KQNCX004, and Guangdong Provincial key S&T Special Project 2017B020235001 and 2019B010943001.

Conflicts of Interest: The authors declare no conflict of interest. The funders had no role in the design of the study; in the collection, analyses, or interpretation of data; in the writing of the manuscript, or in the decision to publish the results.

References

1. He, Y.H.; Hou, X.Q.; Tao, C.H.; Han, F.K. Recrystallization and fatigue fracture of single crystal turbine blades. *Eng. Failure Anal.* **2011**, *18*, 944–949. [[CrossRef](#)]
2. Ma, X.; Shi, H.J.; Gu, J.L.; Yang, Z.; Chen, G.F.; Luesebrink, O.; Harders, H. Influence of surface recrystallization on the low cycle fatigue behavior of a single crystal superalloy. *Fatigue Fract. Eng. Mater. Struct.* **2015**, *38*, 340–351. [[CrossRef](#)]
3. Li, Z.; Xu, Q.; Liu, B. Experimental investigation on recrystallization mechanism of a Ni-base single crystal superalloy. *J Alloy Compd.* **2016**, *672*, 457–469. [[CrossRef](#)]
4. Meng, J.; Jin, T.; Sun, X.; Hu, Z. Effect of surface recrystallization on the creep rupture properties of a nickel-base single crystal superalloy. *Mater. Sci. Eng. A* **2010**, *527*, 6119–6122. [[CrossRef](#)]
5. Xie, G.; Lou, L.H. Influence of the characteristic of recrystallization grain boundary on the formation of creep cracks in a directionally solidified Ni-base superalloy. *Mater. Sci. Eng. A* **2012**, *532*, 579–584. [[CrossRef](#)]
6. Zhang, B.; Lu, X.; Liu, D.L.; Tao, C.H. Influence of recrystallization on high-temperature stress rupture property and fracture behavior of single crystal superalloy. *Mater. Sci. Eng. A* **2012**, *551*, 149–153. [[CrossRef](#)]
7. Zhang, W.F.; Li, Y.J.; Gao, W.; Fan, J.J.; Tao, C.H. Investigation on low cycle fatigue and fracture behaviors of directionally solidified DZ4 superalloy. *Rare Metal Mater. Eng.* **2005**, *34*, 217–220.
8. Bürgel, R.; Portella, P.D.; Preuhs, J. Recrystallization in single crystals of nickel base superalloys. *Superalloys* **2000**, *5*, 229–238.
9. Ma, X.F.; Shi, H.J.; Gu, J.L. In-situ scanning electron microscopy studies of small fatigue crack growth in recrystallized layer of a directionally solidified superalloy. *Mater. Lett.* **2010**, *64*, 2080–2083. [[CrossRef](#)]
10. Shi, H.J.; Zhang, H.F.; Wu, Y.Q. Effect of recrystallization on low-cycle fatigue behavior of DZ4 directionally-solidified superalloy. *Key Eng. Mater.* **2006**, *306*, 175–180. [[CrossRef](#)]
11. Zhao, Y.; Wang, L.; Li, H.Y.; Yu, T.; Liu, Y. Effects of recrystallization on the low cycle fatigue behavior of directionally solidified superalloy DZ40M. *Rare Metals* **2008**, *27*, 425–428. [[CrossRef](#)]
12. Jia, B.; Li, C.G.; Li, H.Y. Influence of recrystallization layer at surface on fatigue behaviors of directionally solidified DZ4 superalloy. *Mater. Eng.* **2008**, *6*, 64–71.
13. Ma, X.; Shi, H.J. In situ SEM studies of the low cycle fatigue behavior of DZ4 superalloy at elevated temperature: Effect of partial recrystallization. *Int. J. Fatigue* **2014**, *61*, 255–263. [[CrossRef](#)]
14. Tomczyk, A.; Seweryn, A.; Grądzka-Dahlke, M. The effect of dynamic recrystallization on monotonic and cyclic behaviour of Al-Cu-Mg alloy. *Materials* **2018**, *11*, 874. [[CrossRef](#)] [[PubMed](#)]
15. Ma, X.F.; Shi, H.J.; Gu, J.L.; Wang, Z.X.; Harders, H.; Malow, T. Temperature effect on low-cycle fatigue behavior of nickel-based single crystalline superalloy. *Acta Mech. Solida Sin.* **2008**, *21*, 289–297. [[CrossRef](#)]
16. *Standard Test Method for Strain-Controlled Fatigue Testing, ASTM E606/E606M-12*; ASTM International: West Conshohocken, PA, USA, 2012.
17. Ma, X.; Wei, D.; Han, Q.; Rui, S. Parametric study of cyclic plasticity behavior in a directionally solidified superalloy with partial recrystallization by crystal plasticity finite element simulation. *J. Mater. Eng. Perform.* **2019**. [[CrossRef](#)]

18. Liu, Y.; Wu, Y.; Wang, J.; Ning, Y. Oxidation behavior and microstructure degeneration of cast Ni-based superalloy M951 at 900 °C. *Appl. Surf. Sci.* **2019**, *479*, 709–719. [[CrossRef](#)]
19. Yi, J.Z.; Torbet, C.J.; Feng, Q.; Pollock, T.M.; Jones, J.W. Ultrasonic fatigue of a single crystal Ni-base superalloy at 1000 °C. *Mater. Sci. Eng. A* **2007**, *443*, 142–149. [[CrossRef](#)]
20. Xu, C.; Nai, Q.L.; Yao, Z.H.; Jiang, H.; Dong, J.X. Grain boundary oxidation effect of GH4738 superalloy on fatigue crack growth. *Acta Metall. Sin.* **2017**, *53*, 1453–1460.
21. Rai, R.K.; Sahu, J.K. Mean-stress and oxidation effects on fatigue behaviour of CM 247 DS LC alloy. *Mater. Sci. Technol.* **2019**, 1–7. [[CrossRef](#)]



© 2019 by the authors. Licensee MDPI, Basel, Switzerland. This article is an open access article distributed under the terms and conditions of the Creative Commons Attribution (CC BY) license (<http://creativecommons.org/licenses/by/4.0/>).